Medical Molecular Morphology (2019) 52:8–14
https://doi.org/10.1007/s00795-018-0194-y

REVIEW

Methods for array tomography with correlative light and electron microscopy

Taro Koike[1] · **Hisao Yamada**[1]

Received: 23 April 2018 / Accepted: 27 May 2018 / Published online: 31 May 2018

Abstract

The three-dimensional ultra-structure is the comprehensive structure that cannot be observed from a two-dimensional electron micrograph. Array tomography is one method for three-dimensional electron microscopy. In this method, to obtain consecutive cross sections of tissue, connected consecutive sections of a resin block are mounted on a flat substrate, and these are observed with scanning electron microscopy. Although array tomography requires some bothersome manual procedures to prepare specimens, a recent study has introduced some techniques to ease specimen preparation. In addition, array tomography has some advantages compared with other three-dimensional electron microscopy techniques. For example, sections on the substrate are stored semi-eternally, so they can be observed at different magnifications. Furthermore, various staining methods, including post-embedding immunocytochemistry, can be adopted. In the present review, the preparation of specimens for array tomography, including ribbon collection and the staining method, and the adaptability for correlative light and electron microscopy are discussed.

Keywords Three-dimensional electron microscopy · Array tomography · Correlative light and electron microscopy · Pre-embedding staining · Post-embedding staining

Introduction

The three-dimensional ultra-structure has been determined with transmission electron microscopy (TEM) for a long time. Serial section TEM (ssTEM) is a technique for three-dimensional microscopy with TEM, where consecutive ultra-thin sections are mounted on TEM grids, and these sections are observed with TEM [1]. These procedures include preparative difficulties as described below. However, recently, back scattered electron imaging with scanning electron microscopy (SEM) has been employed to obtain the three-dimensional ultra-structure. There are mainly two methods to obtain serial cross sections of resin-embedded tissue: "automated method" and "array tomography". Automated methods require repeating 2 step procedures in the SEM chamber; capturing of the block face followed by cutting the block face with a diamond knife or focused ion beam, and these methods are called serial block face SEM (SBF/SEM) or focused ion beam SEM (FIB/SEM), respectively [2, 3].

Array tomography is an imaging technique that was proposed by Micheva and Smith [4]. In this technique, connected consecutive sections, called ribbons, are mounted on a solid substrate, and the sections are observed with fluorescent microscopy and/or SEM. Unlike an automated technique (SBF/SEM and FIB/SEM), array tomography requires some manual procedures to mount the ribbons on the substrate, and to adjust axis of serial image. This manual process needs more time to obtain data set of three-dimensional EM, comparison with automated technique. However, this technique is cost-effective, because specialized expensive machines are not involved. In addition, several studies to improve specimen preparation have been performed. There is also free software to help axis adjustment of serial image [5, 6]. Only array tomography enables post-embedding immunocytochemistry (ICC), because the ribbons for array tomography are mounted on a solid substrate, while, the sections do not remain after capturing in automated techniques. In the present review, ribbon collection methods and staining methods for array tomography are discussed.

✉ Taro Koike
koiket@hirakata.kmu.ac.jp

[1] Department of Anatomy and Cell Science, Kansai Medical University, Shinmachi 2-5-1, Hirakata, Osaka, Japan

Sectioning and preparation of specimens

SBF/SEM and FIB/SEM entail the following advantages regarding sectioning: (1) a large amount of the image is automatically captured; (2) adjustment of each image axis is not needed; and (3) fine z-resolution is obtained (20–25 nm thickness with SBF/SEM [7, 8], few nanometer thickness with FIB/SEM [9, 10]). However, these methods lose the specimen after data acquisition, because sections are removed after being cut off. Furthermore, a smaller area is targeted compared with array tomography.

ssTEM is the oldest and simplest technique for three-dimensional electron microscopy. However, the preparation of specimens is a bottleneck. In this technique, consecutive ultra-thin sections are manually mounted on TEM grids with a single slit. To avoid section loss and/or folding, a well-trained operator is needed. Moreover, the z-resolution of three-dimensional electron microscopy with an ultramicrotome is lower than that of SBF/SEM or FIB/SEM, because it is difficult to prepare the ultra-thin sections, which are thinner than approximately 40 nm. Section thickness is a common problem with array tomography.

Array tomography requires manual procedures to mount the ribbons on the solid substrate; however, various methods have been reported to ease ribbon mounting as described below. These methods allow researchers to choose the area of the section to be investigated depending on their purpose for the experiment.

Automated tape-collecting ultra-microtomy

Automated tape-collecting ultra-microtomy is a semi-automated method to collect consecutive sections. In this technique, consecutive ultra-thin sections are automatically mounted on electrically conductive tape by the use of an automated tape-collecting ultra-microtome (ATUM), although the ATUM is expensive [11, 12]. Unlike SBF/SEM or FIB/SEM, sections made by this technique can be observed repeatedly, which is the same as for ssTEM. Using this method, structure of endoplasmic reticulum has been elucidated [13].

Iron loop method

Koga et al. [14] introduced the simplest method for ribbon collection using an iron loop (Fig. 1a). Several ribbons were obtained on the water boat of a diamond knife, and they were transferred to a glass slide together with water from the boat by the use of an iron loop. Ribbons were dried and attached to a glass slide by heating at 60 °C. The author collected several hundred consecutive ultra-thin sections by repeating this procedure. After electron staining of the sections, the glass slide was cut into smaller sizes, coated with platinum–palladium, and then observed. Using this method, 250 sections are collected from rat cerebellar [15].

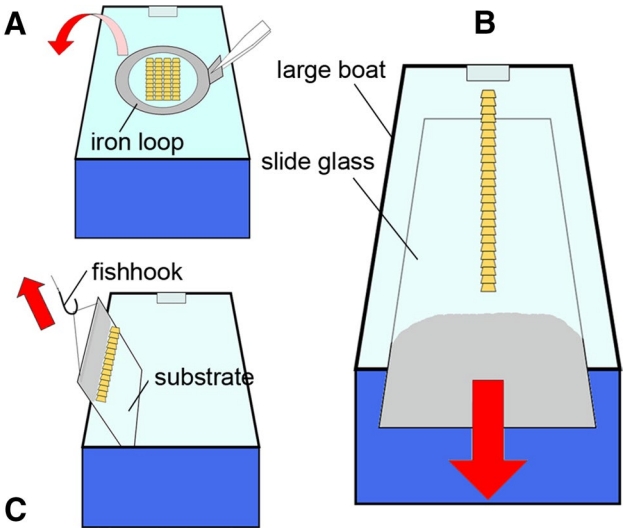

Fig. 1 Ribbon collection methods for array tomography with an iron ring (**a**), large boat (**b**), and crane-like device (**c**). Iron loop or substrate is moved in the direction of the red arrow

Longitudinal ribbon collection with large diamond knife boat

Some researchers employed a diamond knife with a large boat which could mount a whole glass slide [4, 16] (Fig. 1b). A straight long ribbon composed of more than 30 sections was longitudinally pulled out from the water together with the glass slide, and attached to the glass slide by heating at 60 °C. Using this method, a volume image composed of 134 serial sections has been reconstructed [4].

To treat the substrate smoothly in a large boat, a substrate handling device has been developed, because it is difficult to treat the substrate manually and repeatedly. The ribbon can drift or break up on the water owing to waves resulting from movements of the operator's hand. Horstmann et al. [17] developed a substrate positioning device. They built angled forceps attached with a manipulator. The substrate was clipped with the forceps, and the substrate was positioned in the large boat of a diamond knife. The long ribbon was longitudinally pulled out from the water by operating the device. Another researcher built a similar substrate holder [18]. This device enabled for a smoother movement of the substrate in multiple directions. Two-hundred and forty ultra-thin sections were collected with this device [19].

Lateral ribbon collection with a crane-like device

Our previous report introduced a crane-like device to mount ribbons on a small piece of substrate [20] (Fig. 1c). In this method, a 1 × 1 cm square substrate was hung with a fishing line, and the substrate was leant on the side of the knife boat which was a regular size. The other end of the fishing line was connected to the handle of the crane-like device. Ribbons were lined along the substrate, and transversely pulled out from the water together with the substrate by reeling in the fishing line. There was no water turbulence while moving the substrate up or down. By repeating these cycles, ribbons were mounted side by side. This method allowed for mounting approximately 200 sections on a piece of substrate (section size: 500 × 300 µm). The device can be made by recycling material so is inexpensive. Recently, we slightly improved the way to hang the substrate. A fishhook was used to hang the substrate, and the substrate was hung like a handbag (Fig. 1c). Any specific tool was not needed for this improvement. As a result, the substrate could be changed quicker than the previous method, and about 500 sections were mounted on three pieces of the substrate.

Staining

Specimens can be stained according to each technique for section preparation. For SBF/SEM and FIB/SEM, specimens are basically subjected to *en bloc* staining using heavy metals to avoid charging caused by electron beam exposure [21]. Although pre-embedding ICC is also applicable to stain specific molecules for SBF/SEM and FIB/SEM, post-embedding ICC is not, because the sections do not remain after being cut off, as has been mentioned above. In contrast, some staining methods are applicable for array tomography: general electron staining, and pre- and post-embedding ICC (Fig. 2). In this section, staining methods for array tomography are discussed.

General staining method

Ultra-thin sections can be electron stained with acetic uranyl and a lead staining solution on the substrate. If an electrically conductive substrate is used, sections are observed with SEM as it is [22]. When a glass slide is used, an electrically conductive coat is needed [14, 23].

It is possible to stain a specific structure before resin embedding. For example, osmium impregnation has been used to stain Golgi apparatus [14]. This staining deposits a dark high-contrast substance in Golgi apparatus.

Pre-embedding ICC

Pre-embedding ICC is a technique, where tissue is immunocytochemically stained before resin embedding: a tissue slice is obtained; the slice is stained immunocytochemically; the slice is flatly re-embedded in resin; and ribbons are obtained. When 3,3′-diaminobenzidine is used for visualization, an immunoreaction can be detected in a dense substance [24]. This technique enables us to use many kinds of antibodies compared with post-embedding ICC, because the tissue is stained before resin embedding. However, only the slice surface is stained, because antibody infiltration is not high. Thus, a detergent is not able to be used to retain the lipid-derived ultra-structure.

Post-embedding ICC

Post-embedding ICC is a one of the greatest advantages of array tomography compared with the other methods (automated techniques) for three-dimensional electron microscopy, because sections are collected on a solid substrate. In automated techniques, the sections do not remain after capturing. Although ssTEM and automated tape-collecting ultra-microtomy are also applicable for post-embedding ICC, it might be difficult to stain all sections, because the specimen is fragile in ssTEM, and the specimen size is not

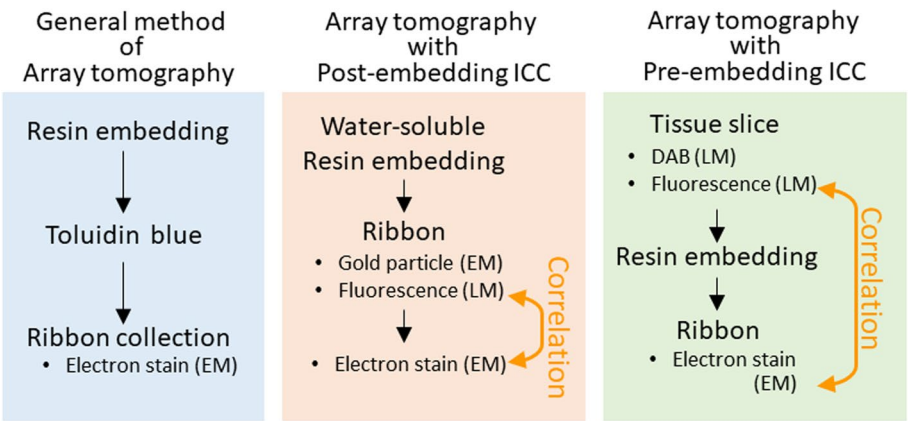

Fig. 2 Flow chart of specimen preparation for array tomography. *AT* array tomography, *LM* light microscopy, *EM* electron microscopy

compact in automated tape-collecting ultra-microtomy. Post-embedding ICC with a colloidal gold labeled antibody is one of the most accepted methods to label molecules. We have confirmed whether ultra-thin sections mounted on a silicon substrate are able to be stained with a gold particle conjugated antibody (Fig. 3b). In this procedure, the

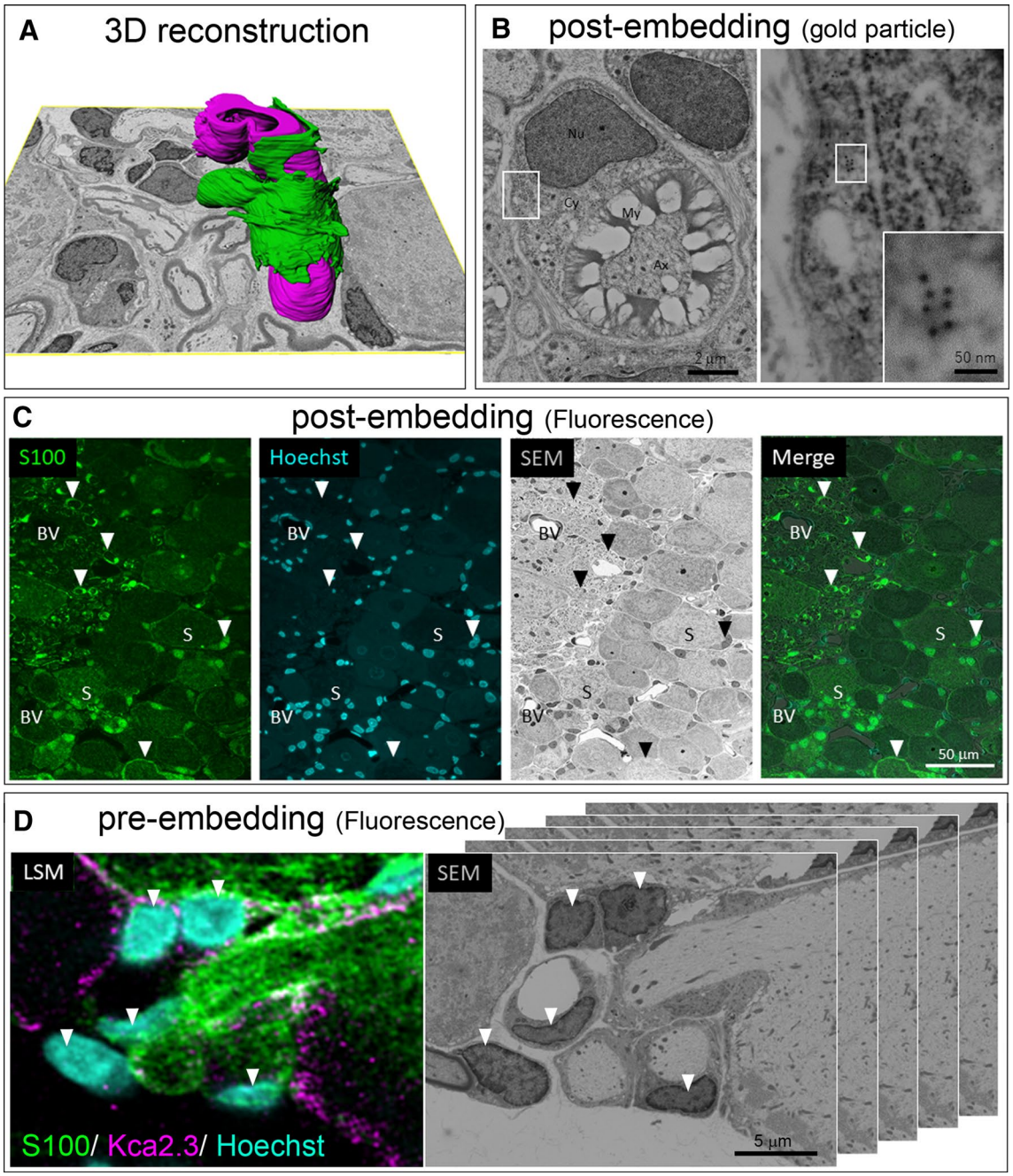

Fig. 3 Micrographs from various staining methods. All specimens are derived from rat dorsal root ganglion. **a** Three-dimensional images made from sections stained with a general electron stain. A myelinating Schwann cell (magenta) and mesenchymal cell (green) are reconstructed. **b** Post-embedding ICC on LR-white embedded tissue. Section was stained with anti-S100 antibody and a 10 nm diameter gold particle conjugated secondary antibody. Boxed areas are enlarged. *Nu* nucleus, *Cy* cytoplasm, *My* myelin sheath, *Ax* axon. **c** Correlative images of the fluorescence micrograph stained with post-embedding ICC and the electron micrograph. Section derived from LR-white resin-embedded tissue was stained with anti-S100 antibody and fluorescent secondary antibody. Arrowheads indicate S100 positive glial cells. *BV* blood vessel; *S* neuronal soma. **d** Correlative images of fluorescence micrograph stained with pre-embedding ICC and electron micrograph. Tissue slice was stained with primary antibodies and fluorescent secondary antibody. Anti-S100, -Kca2.3, and -Hoechst stained neurons and glia, satellite glial cells, and DNA, respectively. Arrowheads indicate nuclei that can be recognized in both images

tissue was embedded in a water-soluble resin. Ribbons were mounted on a silicon substrate, and were soaked in diluted antibody together with the substrate. The specimen was then observed with SEM. The gold particles were able to be clearly detected under SEM. As a modified staining method with a gold labeled antibody, sections can be double stained by sequential immunogold-labeling and silver enhancement. This technique facilitates double staining, because gold particles recognizing different antigens are enhanced by different degrees, even if the species of the primary antibody is the same [25]. It is also known that sections on substrate can be immunoreacted with fluorescent antibodies when water-soluble resin is used [26, 27].

A disadvantage of the post-embedding method is loss of antigenicity, because the tissue is dehydrated with an organic solvent and embedded into the resin before immunocytochemistry. To recover antigenicity, it has been reported that heat antigen retrieval could be helpful [28]. However, heat treatment might cause ribbon shrinkage or detachment of the ribbon from the substrate.

CLEM

Correlative light and electron microscopy (CLEM) is a technique, where correlative images of light and electron micrographs are obtained [29, 30]. Recently, CLEM for biological tissue combined with fluorescent immunocytochemistry has been developed [31–35]. In this section, CLEM combined with array tomography is discussed.

CLEM with post-embedding ICC

This technique basically requires the following procedures: (1) ribbons derived from water-soluble resin are stained with a fluorescent antibody, and captured with fluorescence microscopy; (2) ribbons are electron stained, the region that was captured with fluorescence microscopy is re-captured with SEM; and (3) both fluorescence and electron microscopy images are adjusted for CLEM. Using this technique, the distribution of 7 kinds of proteins on a synapse was investigated together with the three-dimensional ultra-structure [36]. Thus, resin-embedded sections were subjected to multi-label ICC twice by the use of the antibody elution technique [37]. We also confirmed that fluorescence image can be obtained with epifluorescence microscopy even if sections are mounted on a silicon wafer substrate (Fig. 3c).

It is also known that neuro tracers derived from dextran-coupled fluorophores can be re-labeled by ICC [38, 39]. Tissue preparation for EM significantly reduces fluorescence. Therefore, the neuro tracers can be re-labeled, and ultra-structure of the tracer positive neuron can be observed.

ICC with fluoronanogold allows for signal detection with not only fluorescence microscopy but also electron microscopy. This method is helpful for obtaining a correlative image, because immunoreaction can be observed both light and electron microscopy [40].

Part of a section could be stained when the iron loop method is used [15]. Two sections were obtained in the middle of the ribbon collection, and a hormone was immunocytochemically stained to determine the cell type. The adjacent images derived from ICC and SEM were then correlated.

CLEM with pre-embedding ICC

In this method, a specimen is light-microscopically visualized by fluorescent reagents, and then the region of interest is captured with confocal laser scanning microscopy. The specimen is re-embedded into the resin, and a series of ultra-thin sections is obtained. Finally, electron microscopy images that correlate with the fluorescence image are obtained by SEM. Although, it has been reported that pre-embedding staining method is applicable for automated three-dimensional EM technique [41–43], we also confirmed whether the technique can be applicable for array tomography with tissue slice (Fig. 3d). Although, the exact molecular localization is not observed, it is sufficient to identify cell types by the use of cell-type specific antibodies.

Efficient three-dimensional correlative image with these methods described above will lead us towards a comprehensive understanding of the ultra-structure and its function.

Conclusions

Array tomography is a technique to observe the three-dimensional ultra-structure. Although manual procedures are needed to prepare the specimen, this technique is inexpensive. Moreover, various cytochemical staining methods, including post-embedding immunocytochemistry, are applicable. Array tomography is an effective way to reveal the three-dimensional ultra-structure with molecular information.

Acknowledgements We thank Edanz Group (http://www.edanzediting.com/ac) for editing a draft of this manuscript.

Funding This study was supported in part by Grants-in-Aid for Scientific Research (C) from the Japan Society for the Promotion of Science [16k08480 to H.Y.], The Science Research Promotion Fund from the Proportion and Mutual Aid Corporation for Private Schools of Japan [to T.K.].

References

1. White JG, Southgate E, Thomson JN, Brenner S (1986) The structure of the nervous system of the nematode Caenorhabditis elegans. Philos Trans R Soc Lond B Biol Sci 314:1–340
2. Denk W, Horstmann H (2004) Serial block-face scanning electron microscopy to reconstruct three-dimensional tissue nanostructure. PLoS Biol 2:e329
3. Knott G, Marchman H, Wall D, Lich B (2008) Serial section scanning electron microscopy of adult brain tissue using focused ion beam milling. J Neurosci 28:2959–2964
4. Micheva KD, Smith SJ (2007) Array tomography: a new tool for imaging the molecular architecture and ultrastructure of neural circuits. Neuron 55:25–36
5. Cardona A, Saalfeld S, Schindelin J, Arganda-Carreras I, Preibisch S, Longair M, Tomancak P, Hartenstein V, Douglas RJ (2012) TrakEM2 software for neural circuit reconstruction. PLoS One 7:e38011
6. Saalfeld S, Fetter R, Cardona A, Tomancak P (2012) Elastic volume reconstruction from series of ultra-thin microscopy sections. Nat Methods 9:717–720
7. Briggman KL, Helmstaedter M, Denk W (2011) Wiring specificity in the direction-selectivity circuit of the retina. Nature 471:183–188
8. Vihinen H, Belevich I, Jokitalo E (2013) Three dimensional electron microscopy of cellular organ elles by serial block face SEM and ET. Microsc anal 27:7–10
9. Kopek BG, Shtengel G, Xu CS, Clayton DA, Hess HF (2012) Correlative 3D superresolution fluorescence and electron microscopy reveal the relationship of mitochondrial nucleoids to membranes. Proc Natl Acad Sci USA 109:6136–6141
10. Wei D, Jacobs S, Modla S, Zhang S, Young CL, Cirino R, Caplan J, Czymmek K (2012) High-resolution three-dimensional reconstruction of a whole yeast cell using focused-ion beam scanning electron microscopy. Biotechniques 53:41–48
11. Hayworth KJ, Morgan JL, Schalek R, Berger DR, Hildebrand DG, Lichtman JW (2014) Imaging ATUM ultrathin section libraries with WaferMapper: a multi-scale approach to EM reconstruction of neural circuits. Front Neural Circuits 8:68
12. Hayworth KJ, Kasthuri N, Schalek R, Lichtman JW (2006) Automating the collection of ultrathin serial sections for large volume TEM reconstructions. Microsc Microanal 12:86–87
13. Terasaki M, Shemesh T, Kasthuri N, Klemm RW, Schalek R, Hayworth KJ, Hand AR, Yankova M, Huber G, Lichtman JW, Rapoport TA, Kozlov MM (2013) Stacked endoplasmic reticulum sheets are connected by helicoidal membrane motifs. Cell 154:285–296
14. Koga D, Kusumi S, Ushiki T (2016) Three-dimensional shape of the Golgi apparatus in different cell types: serial section scanning electron microscopy of the osmium-impregnated Golgi apparatus. Microscopy (Oxf) 65:145–157
15. Koga D, Kusumi S, Ushiki T, Watanabe T (2017) Integrative method for three-dimensional imaging of the entire Golgi apparatus by combining thiamine pyrophosphatase cytochemistry and array tomography using backscattered electron-mode scanning electron microscopy. Biomed Res 38:285–296
16. Blumer MJ, Gahleitner P, Narzt T, Handl C, Ruthensteiner B (2002) Ribbons of semithin sections: an advanced method with a new type of diamond knife. J Neurosci Methods 120:11–16
17. Horstmann H, Korber C, Satzler K, Aydin D, Kuner T (2012) Serial section scanning electron microscopy (S3EM) on silicon wafers for ultra-structural volume imaging of cells and tissues. PLoS One 7:e35172
18. Spomer W, Hofmann A, Wacker I, Ness L, Brey P, Schröder R R, Gengenbach U (2015) Advanced substrate holder and multi-axis manipulation tool for ultramicrotomyAdvanced substrate holder and multi-axis manipulation tool for ultramicrotomy. Microsc Microanal 21:1277–1278
19. Wacker I, Spomer W, Hofmann A, Thaler M, Hillmer S, Gengenbach U, Schroder RR (2016) Hierarchical imaging: a new concept for targeted imaging of large volumes from cells to tissues. BMC Cell Biol 17:38
20. Koike T, Kataoka Y, Maeda M, Hasebe Y, Yamaguchi Y, Suga M, Saito A, Yamada H (2017) A Device for Ribbon Collection for Array Tomography with Scanning Electron Microscopy. Acta Histochem Cytochem 50:135–140
21. Tapia JC, Kasthuri N, Hayworth KJ, Schalek R, Lichtman JW, Smith SJ, Buchanan J (2012) High-contrast en bloc staining of neuronal tissue for field emission scanning electron microscopy. Nat Protoc 7:193–206
22. Wacker I, Chockley P, Bartels C, Spomer W, Hofmann A, Gengenbach U, Singh S, Thaler M, Grabher C, Schroder RR (2015) Array tomography: characterizing FAC-sorted populations of zebrafish immune cells by their 3D ultrastructure. J Microsc 259:105–113
23. Shodo R, Hayatsu M, Koga D, Horii A, Ushiki T (2017) Three-dimensional reconstruction of root cells and interdental cells in the rat inner ear by serial section scanning electron microscopy. Biomed Res 38:239–248
24. Armstrong WE, Rubrum A, Teruyama R, Bond CT, Adelman JP (2005) Immunocytochemical localization of small-conductance, calcium-dependent potassium channels in astrocytes of the rat supraoptic nucleus. J Comp Neurol 491:175–185
25. Yi H, Leunissen J, Shi G, Gutekunst C, Hersch S (2001) A novel procedure for pre-embedding double immunogold-silver labeling at the ultrastructural level. J Histochem Cytochem 49:279–284
26. Koffie RM, Meyer-Luehmann M, Hashimoto T, Adams KW, Mielke ML, Garcia-Alloza M, Micheva KD, Smith SJ, Kim ML, Lee VM, Hyman BT, Spires-Jones TL (2009) Oligomeric amyloid beta associates with postsynaptic densities and correlates with excitatory synapse loss near senile plaques. Proc Natl Acad Sci U S A 106:4012–4017
27. Soiza-Reilly M, Commons KG (2011) Quantitative analysis of glutamatergic innervation of the mouse dorsal raphe nucleus using array tomography. J Comp Neurol 519:3802–3814
28. Yamashita S (2010) The post-embedding method for immunoelectron microscopy of mammalian tissues: a standardized procedure based on heat-induced antigen retrieval. Methods Mol Biol 657:237–248
29. Nakai Y, Iwashita T (1976) Correlative light and electron microscopy of the frog adrenal gland cells using adjacent epon-embedded sections. Arch Histol Jpn 39:183–191
30. Watari N, Tsukagoshi N, Honma Y (1970) The correlative light and electron microscopy of the islets of Langerhans in some lower vertebrates. Arch Histol Jpn 31:371–392
31. de Boer P, Hoogenboom JP, Giepmans BN (2015) Correlated light and electron microscopy: ultrastructure lights up! Nat Methods 12:503–513
32. Kim D, Deerinck TJ, Sigal YM, Babcock HP, Ellisman MH, Zhuang X (2015) Correlative stochastic optical reconstruction microscopy and electron microscopy. PLoS One 10:e0124581
33. Koga D, Kusumi S, Bochimoto H, Watanabe T, Ushiki T (2015) Correlative light and scanning electron microscopy for observing the three-dimensional ultrastructure of membranous cell organelles in relation to their molecular components. J Histochem Cytochem 63:968–979
34. Saitoh S, Ohno N, Saitoh Y, Terada N, Shimo S, Aida K, Fujii H, Kobayashi T, Ohno S (2018) improved serial sectioning techniques for correlative light-electron microscopy mapping of human langerhans islets. Acta Histochem Cytochem 51:9–20
35. Sengle G, Tufa SF, Sakai LY, Zulliger MA, Keene DR (2013) A correlative method for imaging identical regions of samples

by micro-CT, light microscopy, and electron microscopy: imaging adipose tissue in a model system. J Histochem Cytochem 61:263–271
36. Collman F, Buchanan J, Phend KD, Micheva KD, Weinberg RJ, Smith SJ (2015) Mapping synapses by conjugate light-electron array tomography. J Neurosci 35:5792–5807
37. Micheva KD, Busse B, Weiler NC, O'Rourke N, Smith SJ (2010) Single-synapse analysis of a diverse synapse population: proteomic imaging methods and markers. Neuron 68:639–653
38. Oberti D, Kirschmann MA, Hahnloser RH (2010) Correlative microscopy of densely labeled projection neurons using neural tracers. Front Neuroanat 4:24
39. Oberti D, Kirschmann MA, Hahnloser RH (2011) Projection neuron circuits resolved using correlative array tomography. Front Neurosci 5:50
40. Koga D, Kusumi S, Shodo R, Dan Y, Ushiki T (2015) High-resolution imaging by scanning electron microscopy of semithin sections in correlation with light microscopy. Microscopy (Oxf) 64:387–394
41. Beckwith MS, Beckwith KS, Sikorski P, Skogaker NT, Flo TH, Halaas O (2015) Seeing a mycobacterium-infected cell in nanoscale 3D: correlative imaging by light microscopy and FIB/SEM tomography. PLoS One 10:e0134644
42. Booth DG, Beckett AJ, Molina O, Samejima I, Masumoto H, Kouprina N, Larionov V, Prior IA, Earnshaw WC (2016) 3D-CLEM Reveals that a Major Portion of Mitotic Chromosomes Is Not Chromatin. Mol Cell 64:790–802
43. Shtengel G, Wang Y, Zhang Z, Goh WI, Hess HF, Kanchanawong P (2014) Imaging cellular ultrastructure by PALM, iPALM, and correlative iPALM-EM. Methods Cell Biol 123:273–294